

resembling the ruffling of the skeleton as a mechanism for effecting inversion of five-coordinate porphyrins with sizable out-of-plane displacements, as characterized in static structures.

The rate constants in Table I and the kinetic parameters in Table II represent inversion as induced by associative halide exchange occurring exclusively via an SN2 mechanism. Any halide exchange occurring on the same side of the porphyrin goes undetected in the NMR method¹⁵ employed here. Thus the present system represents one of the most thoroughly characterized cases of axial ligand lability in metalloporphyrins.¹⁹

Acknowledgment. The authors are indebted to Professor F. Basolo for a stimulating discussion, to Professor Innhofen for a gift of OEP, and to the National Institute of Health (HL-16087) for support of this research.

References and Notes

- Fellow of the Alfred P. Sloan Foundation.
- (a) J. L. Hoard, *Science*, **174**, 1295 (1971); (b) J. L. Hoard, M. J. Hamor, T. A. Hamor, and W. S. Caughey, *J. Am. Chem. Soc.*, **87**, 2312 (1965); D. F. Koenig, *Acta Crystallogr.*, **18**, 663 (1965).
- J. L. Hoard, C. H. Cohen, and M. D. Glick, *J. Am. Chem. Soc.*, **89**, 1992 (1967).
- D. M. Collins, R. Countryman, and J. L. Hoard, *J. Am. Chem. Soc.*, **94**, 2066 (1972).
- L. J. Rabinovich, A. Bloom, and J. L. Hoard, *J. Am. Chem. Soc.*, **94**, 2073 (1972).
- M. F. Perutz, *Nature (London)*, **228**, 726 (1970).
- J. C. Kendrew, *Science*, **139**, 1259 (1963); R. Huber, O. Epp, and H. Formanek, *J. Mol. Biol.*, **42**, 591 (1971).
- M. F. Perutz and L. F. TenEyck, *Cold Spring Harbor Symp. Quant. Biol.*, **36**, 295 (1971); M. F. Perutz, *Nature (London)*, **237**, 495 (1972).
- R. J. P. Williams, *Cold Spring Harbor Symp. Quant. Biol.*, **36**, 53 (1971).
- E. B. Fleischer, *Acc. Chem. Res.*, **3**, 105 (1970).
- D. M. Collins, W. R. Sheidt, and J. L. Hoard, *J. Am. Chem. Soc.*, **94**, 6689 (1972).
- A. L. Stone and E. B. Fleischer, *J. Am. Chem. Soc.*, **90**, 2735 (1968).
- T. A. Hamor, W. S. Caughey, and J. L. Hoard, *J. Am. Chem. Soc.*, **87**, 2305 (1965).
- M. Zerner, M. Gouterman, and H. Kobayashi, *Theor. Chim. Acta*, **6**, 363 (1966).
- G. N. La Mar, *J. Am. Chem. Soc.*, **95**, 1662 (1973).
- G. N. La Mar, *Pure Appl. Chem.*, **40**, 13 (1974).
- G. N. La Mar, G. R. Eaton, R. H. Holm, and F. A. Walker, *J. Am. Chem. Soc.*, **95**, 63 (1973).
- F. A. Walker and G. N. La Mar, *Ann. N.Y. Acad. Sci.*, **206**, 328 (1973).
- G. N. La Mar and F. A. Walker, *J. Am. Chem. Soc.*, **94**, 8607 (1972).
- E. B. Fleischer, S. Jacobs, and L. Mestichelli, *J. Am. Chem. Soc.*, **90**, 2527 (1968); G. B. Kolski and R. A. Plane, *ibid.*, **94**, 3740 (1972); B. B. Hasinoff, H. B. Dunford, and D. G. Horne, *Can. J. Chem.*, **47**, 3225 (1969); N. S. Angerman, B. B. Hasinoff, H. B. Dunford, and R. B. Jordan, *ibid.*, **47**, 3217 (1969); J. Hodgkinson and R. B. Jordan, *J. Am. Chem. Soc.*, **95**, 763 (1973); H. A. Degani and D. Fiat, *ibid.*, **93**, 4281 (1971).
- C. G. Grimes and R. G. Pearson, *Inorg. Chem.*, **13**, 970 (1974); C. G. Grimes, Ph.D. Thesis, Northwestern University, 1973.
- A. D. Adler, F. R. Longo, F. Kampas, and J. Kim, *J. Inorg. Nucl. Chem.*, **32**, 2443 (1970).
- G. N. La Mar and F. A. Walker, *J. Am. Chem. Soc.*, **95**, 6950 (1973).
- M. F. Reich and I. A. Cohen, *J. Inorg. Nucl. Chem.*, **32**, 343 (1970).
- C. R. Witschanke and C. A. Kraus, *J. Am. Chem. Soc.*, **69**, 2473 (1947).
- This program was kindly provided by L. H. Pignolet.
- J. A. Pople, W. G. Schneider, and H. J. Bernstein, "High Resolution Nuclear Magnetic Resonance", McGraw-Hill, New York, N.Y., 1959, Chapter 10.
- G. N. La Mar and E. O. Sherman, *J. Am. Chem. Soc.*, **92**, 2691 (1970).
- M. Momenteau, J. Mispelter, and D. Lexa, *Biochim. Biophys. Acta*, **322**, 38 (1973).
- J. T. Thomas and D. F. Evans, *J. Phys. Chem.*, **74**, 3812 (1970); M. A. Matesich, J. A. Nadas, and D. F. Evans, *ibid.*, **74**, 4568 (1970); D. F. Evans, J. Thomas, J. A. Nadas, and M. A. Matesich, *ibid.*, **75**, 1714 (1971).
- The large uncertainty in ΔH^\ddagger for inversion in the case of *p*-CH₃-TPPFeCl is due to the fact that at the temperatures where inversion kinetics were determined, the two *m*-H protons can also average by phenyl rotation (G. R. Eaton and S. S. Eaton, *J. Am. Chem. Soc.*, **97**, 3660 (1975)). This process is concentration independent so that it can be clearly distinguished from inversion. The two processes overlap in the temperature range 20–30 °C. Although attempts were made to correct for phenyl rotation kinetics, the inability to clearly define the phenyl rotation kinetic parameter introduces sizable uncertainties in the line broadening due to inversion.
- There is some evidence that these porphyrin dimerize in CD₂Cl₂ (R. V. Snyder and G. N. La Mar, unpublished observations). Thus the molecularity of the associative inversion with respect to Bu₄N⁺X⁻ is 1.0, but only ~0.9 with respect to porphyrin. This small extent of dimerization at 25°, however, is unlikely to affect the relative rates of inversion for different parasubstituents.
- J. E. Falk and J. N. Phillips, *Nature (London)*, **212**, 153 (1966); W. S. Caughey, W. Y. Fujimoto, and B. P. Johnson, *Biochemistry*, **5**, 3830 (1966).
- In acetone, addition of HgI₂ to *p*-CH₃-TPPFeI caused a decrease in the 512-nm band and the growth of a new peak at 527 nm. Subsequent addition of Bu₄N⁺I⁻ reversed the process.
- The authors are indebted to F. Basolo for this suggestion.
- F. Gaizer and G. Johansson, *Acta Chem. Scand.*, **22**, 3013 (1968); M. A. Hooper and D. W. James, *Aust. J. Chem.*, **24**, 1345 (1971).
- G. B. Deacon, *Rev. Pure Appl. Chem.*, **13**, 189 (1963).
- S. S. Eaton and G. R. Eaton, *J. Chem. Soc., Chem. Commun.*, 576 (1974).
- F. A. Cotton and G. Wilkinson, "Advanced Inorganic Chemistry", Interscience, New York, N.Y., 1966.

Solute Complexes in Aqueous Gadolinium(III) Chloride Solutions

Marcus L. Steele and D. L. Wertz*

Contribution from the Department of Chemistry, University of Southern Mississippi, Hattiesburg, Mississippi 39401. Received September 16, 1975

Abstract: The structure of the average solute species in two concentrated aqueous solutions of GdCl₃, with and without added hydrochloric acid, has been measured. In each solution Gd³⁺ has 8 (±0.2) nearest neighbors. The average solute species are Gd(H₂O)₈³⁺ in the aqueous solution and Cl₂Gd(H₂O)₆⁺ in the solution in which hydrochloric acid is the solvent. The average Gd–O nearest neighbor distance has been measured to be 2.37 (±0.02) Å, and the nearest neighbor Gd–Cl distance has been calculated to be ca. 2.8 Å. The ion-pair Gd³⁺–Cl distance ranges from 4.8 to 5.0 Å. On the average, dichlorohexaquo-gadolinium(III) appears to be pseudocubic (*D*_{3h}), but no satisfactory solute model of Gd(H₂O)₈³⁺ has been found.

Introduction

Interest in the aqueous solution chemistry of Gd³⁺ has dramatically increased in the past few years because of its frequent use as a lanthanide shift reagent,¹ a probe in studying metal-amino acid complexes,^{2,3} and because of the "gadolinium break"⁴ observed in many thermodynamic measurements of solutions containing various lanthanide salts. Notwithstanding, the solution chemistry of Gd³⁺ has not been thoroughly studied and is not well understood. As noted by Mioduski and Siekierski,⁵ considerable question still exists regarding the coordination number(s) of the various lan-

thanide break⁴ observed in many thermodynamic measurements of solutions containing various lanthanide salts. Notwithstanding, the solution chemistry of Gd³⁺ has not been thoroughly studied and is not well understood. As noted by Mioduski and Siekierski,⁵ considerable question still exists regarding the coordination number(s) of the various lan-

Table I. Solution Compositions

Soln	Molality, mol/kg	Mole fractions				Density, g/ml
		Gd	Cl	O	H	
A ^a	2.66	0.015	0.045	0.313	0.627	1.58
B ^b	1.55	0.010	0.060	0.300	0.630	1.34

^a The solvent is distilled deionized water. The stoichiometric ratio of chloride/gadolinium is 3:1. ^b The solvent is 10 N hydrochloric acid. The stoichiometric ratio of chloride/gadolinium is 6:1.

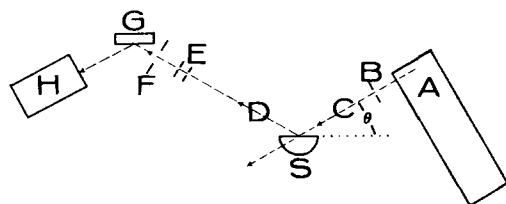


Figure 1. Schematic of the θ - θ diffractometer. The figure is not drawn to scale, and the divergence-convergence of the x-ray beam is not shown. A, X-ray tube; B, exit slit; C, incident beam; D, scattered beam; E, receiving slits; F, antiscatter slit; G, crystal monochromator; H, detector; S, sample; θ , scattering angle.

thanides in aqueous solutions⁶⁻¹² and whether the coordination number(s) change as a function of the lanthanide cation and/or other chemical parameters in such solutions.

Spedding and Mundy¹³ have shown that water molecules (in a solvent of 95% water and 5% deuterium oxide) are affected differently by Gd^{3+} than by La^{3+} when the lanthanide is introduced as LnCl_3 . These findings are consistent with the fact that La^{3+} is nine-coordinated in $\text{LaCl}_3 \cdot 7\text{H}_2\text{O}$,¹⁴ but that Gd^{3+} is eight-coordinated in $\text{GdCl}_3 \cdot 6\text{H}_2\text{O}$.¹⁵ However, it has recently been shown that La^{3+} is eight-coordinated in aqueous solutions of LaCl_3 ¹⁶ and LaBr_3 ,¹⁷ and Morgan⁹ has suggested that in aqueous solutions of $\text{Gd}(\text{ClO}_4)_3$, Gd^{3+} is either eight- or nine-coordinated. The accumulation of thermodynamic,^{4,5,18-25} electrochemical,²⁶⁻³⁰ spectra,³¹⁻³⁶ and/or formation constant studies³⁷⁻⁴⁰ have not led to definitive assignments of the coordination number(s) or to understanding of the coordination details of the various lanthanides in solutions.

In an attempt to determine the coordination details of Gd^{3+} in very concentrated aqueous solutions, we have examined two aqueous solutions of GdCl_3 , with and without added hydrochloric acid, via x-ray diffraction methods utilizing Mo $K\alpha$ x-rays.

Experimental Section

Solutions were prepared by weight from predried anhydrous GdCl_3 . Densities were measured with a specific gravity bulb. Solution compositions are shown in Table I. Each solution was loaded into a Teflon sample holder, which had a window covered by a 1.0-mil Mylar film, and an x-ray diffraction pattern was obtained using the reflection method.⁴¹ Scattered intensities were collected using our θ - θ diffractometer (Figure 1) as counts per preset time as a function of the scattering angle from $s = 1.23$ to 15.09 \AA^{-1} ($s = 4\pi\lambda^{-1} \sin \theta$) at increments in θ of 0.25° . At least three runs over the entire angular range were made for each solution. The average intensity at each scattering point was used in subsequent calculations. For these solutions the maximum value of $\sigma^{42} < 1\%$, and σ is significantly lower at most of the 219 data points at which data were collected.

The scattered intensity was corrected for background (ca. 5 cpm), for polarization,⁴³ sample penetration,⁴⁴ multiple scattering,⁴⁵ and, after inclusion of a monochromator discrimination function, Compton scattering.⁴⁶ The corrected intensity, e.g., the coherent intensity curve $I(s)$, was then tentatively computer fitted to $\sum x_i f_i^2(s)$,⁴⁷ according to the methods of Lawrence and Kruh.⁴⁸ Final fitting of $I(s)$ to

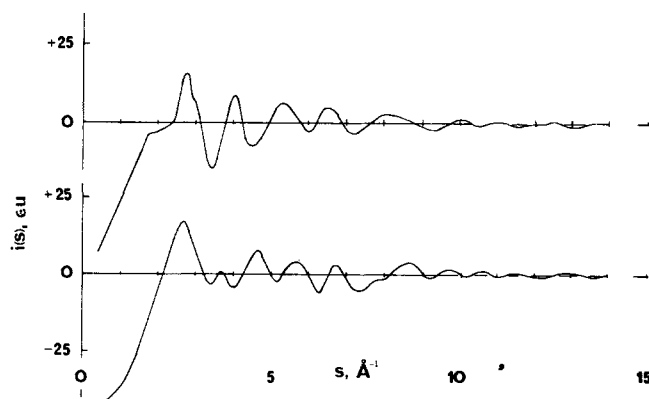


Figure 2. The $i(s)$ functions for the solutions.

Table II. Summary of the ARDF's

	Soln A	Soln B
P1, \AA	2.37	2.48
P1A, e^2	114	105
Area per Gd, $^a e^2$	7.6×10^3	1.05×10^4
P2, \AA	3.2	3.2
P3, \AA	3.9	4.0
P4, \AA	4.8	5.0
P5, \AA	5.9	<i>b</i>
P6, \AA	6.8	6.9

^a The area per gadolinium = P1A/mol fraction of gadolinium.

^b This peak is barely discernible in the ARDF of solution B at 5.8 \AA .

$\sum x_i f_i^2(s)$ was performed by a method similar to that used by Konnerth and Karle.⁴⁹ Atomic radial distribution functions (ARDF's) were calculated at increments in Δr of 0.01 and 0.05 \AA by⁴¹

$$D(r) = 4\pi r^2 \rho_0 + (2r/\pi) \int [s i(s)] [M(s)] [\sin sr] ds$$

With this method $D(r)$ provides a weighted measure of the probability of finding atom pairs in the solution separated by a distance between r and $r + dr$, ρ_0 is the bulk density of the solution, $s i(s) = s [I_{\text{coh}}(s) - \sum x_i f_i^2(s)]$, and

$$M(s) = \{ [\sum x_i f_i(0) / \sum x_i f_i(s)] \}^2 \{ \exp(-bs^2) \} \text{USF}$$

USF is a unit step function which terminates the integral at $s_{\text{max}} = 15 \text{ \AA}^{-1}$.

Shown in Figure 2 are the $i(s)$ functions for the solutions, and in Figure 3 are the ARDF's obtained with $b = 0.010$. Shown in Figure 4 are the atom-pair correlation functions (APCF) (e.g., $g(r) = D(r)/4\pi r^2 \rho_0$) obtained for the solutions. Summarized in Table II are the ARDF's.

The area under the first peak in each ARDF was determined via repeated graphical integration, so that deviation from the mean area of each first peak was $< 2\%$ of the peak area.

For each solution the area anticipated for one Gd-Cl pair ($A_{\text{Gd-Cl}}$) and that for one Gd-O pair ($A_{\text{Gd-O}}$) were calculated by the method of Wasser and Schomaker.⁵⁰ $A_{\text{Gd-O}} = 950$ and $A_{\text{Gd-Cl}} = 2400 e^2$.

Both the position of and the area under the first peak have been

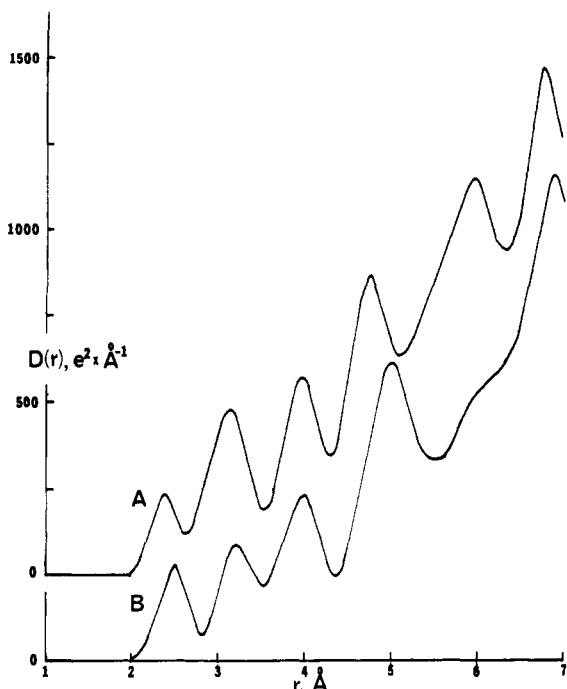


Figure 3. The ARDF's of the two solutions with $b = 0.01$.

utilized to determine the average inner-sphere coordination of Gd^{3+} in each solution by

$$P1 \approx n_1 d_{\text{Gd-O}} + n_2 Q d_{\text{Gd-Cl}} \quad (1)$$

$$P1A = n_1 \cdot 950 \text{ e}^2 + n_2 \cdot 2400 \text{ e}^2 \quad (2)$$

In these equations, n_1 and n_2 are the average number of Gd-O and Gd-Cl contacts per Gd^{3+} , $d_{\text{Gd-X}}$ are the Gd-O and Gd-Cl distances as determined in crystals, $Q \approx A_{\text{Gd-Cl}}/A_{\text{Gd-O}}$, P1 is the location of the first peak, and P1A is the area under the peak in each ARDF.

Based upon this method of correlating the primary peak in the ARDF with the average inner-sphere coordination of a cation, the uncertainty in the determination of the coordination number of the cation is not significantly larger than the uncertainty in the area under the primary peak. In several other solutions,⁵¹ the maximum uncertainty in the coordination number of the cation appears to be less than 0.2, and this is consistent with error estimates by Konnert and Karle.⁴⁹

Results and Discussion

The ARDF's obtained for the two solutions are generally similar, indicating that the average coordination of Gd^{3+} in these solutions is similar. However, as the stoichiometric ratio of chloride/gadolinium increases, the maximum of the first peak shifts from ca. 2.37 to ca. 2.48 Å, P4 shifts from 4.8 to 5.0 Å, and P5, a large peak in the ARDF of solution A, becomes barely discernible in the ARDF of solution B. The areas per gadolinium are $7.60 \times 10^3 \text{ e}^2$ in solution A and $1.05 \times 10^4 \text{ e}^2$ in solution B. The shift in the location of P1 and the increase in the area per gadolinium indicate that there is significantly more inner-sphere Gd-Cl bonding in solution B than in solution A.

Solution A. The location of the first peak (2.37 Å) is consistent with Gd-O inner-sphere bonding,^{15,52,53} and the area per gadolinium indicates that each Gd^{3+} has, on the average, ca. eight nearest oxygen (water) neighbors.⁵⁴ An eight-coordinated species is consistent with the results obtained from a study of aqueous LaCl_3 solutions^{16,17} and the coordination of Gd^{3+} in crystalline $\text{GdCl}_3 \cdot 6\text{H}_2\text{O}$.¹⁵ Though P1A can be related to a six-coordinated model, this model requires extensive Gd-Cl as well as Gd-O inner-sphere bonding. The location of P1 indicates that inner-sphere Gd-Cl bonding is unimportant in this solution.

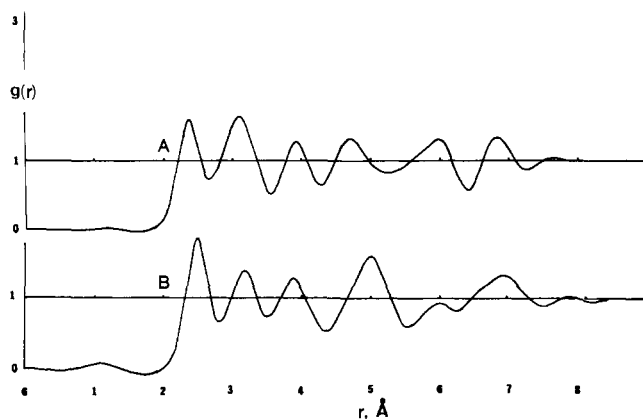


Figure 4. The APCF's of the two solutions. For each solution $g(r) = D(r)/4\pi r^2 \rho_0$.

Solution B. The similarities of the two ARDF's indicate that Gd^{3+} is, on the average, eight-coordinated in solution B as well, with P1 again describing the inner-sphere Gd-ligand interactions. From evaluation of eq 2, the area per gadolinium is consistent with $n_1 \approx 6.0$ and $n_2 \approx 2.0$; i.e., the average solute species in solution B is approximately $\text{Cl}_2\text{Gd}(\text{H}_2\text{O})_6^+$.⁵⁵ From evaluation of eq 1 and assuming the Gd-O distance is 2.37 Å, the Gd-Cl (inner-sphere) bond distance is estimated to be ca. 2.8 Å. Both the average complex, $\text{Cl}_2\text{Gd}(\text{H}_2\text{O})_6^+$, and the inner-sphere Gd-Cl distance, ca. 2.8 Å, are consistent with the complex ion found in crystalline $\text{GdCl}_3 \cdot 6\text{H}_2\text{O}$.¹⁵

The Second Peak. In aqueous solutions which contain chloride,^{16,51,56-62} hydrogen-bonded Cl-O interactions occur at 3.15-3.30 Å. The ARDF's of both of these solutions exhibit a peak at this distance. Consequently, the existence of P2 neither supports nor eliminates any coordination models, since it is due primarily, if not totally, to hydrogen-bonded Cl-O interactions.

Speculations Concerning the Remaining Peaks. Since in aqueous LaCl_3 ¹⁶ and ErCl_3 solutions,⁶ ion-pair $\text{Ln} \cdots \text{Cl}$ interactions occur at 4.7 and 4.6 Å, respectively, P4 in each solution has been assigned to ion-pair $\text{Gd} \cdots \text{Cl}$ interactions. This peak occurs at 4.8 Å in solution A and 5.0 Å in solution B, where inclusion of chlorides into the inner sphere causes the average ion-pair $\text{Gd} \cdots \text{Cl}$ distance to be increased. Zachariasen et al. find this interaction at a distance comparable to 5.0 Å in crystalline $\text{GdCl}_3 \cdot 6\text{H}_2\text{O}$, which contains two inner-sphere chlorides.¹⁵

Solute Modeling. A pseudocubic model of $\text{Cl}_2\text{Gd}(\text{H}_2\text{O})_6^+$ accounts for the ARDF obtained for solution B if it assumed that the outer-sphere chlorides occupy sites adjacent to the faces of the inner-sphere complex. The nonbonded distances consistent with this model are shown in Table III, and the model is shown in Figure 5. The peak observed at 3.2 Å may be attributed to nonbonded Cl...O interactions as well as to hydrogen-bonded Cl-O interactions. The peak at 4.0 Å may be attributed to nonbonded Cl...O interactions (at 4.0 and 4.1 Å), to nonbonded O...O interactions (at 3.9 Å) and to nonbonded Cl...Cl interactions (at 4.1 Å). The peak observed at 5.0 Å may be attributed primarily to outersphere Gd-Cl interactions and also to nonbonded O...O interactions. The peak at 6.9 Å may be attributed to nonbonded Cl...O and nonbonded Cl...Cl interactions.

We have considered several other stereochemical arrangements of this solute species, i.e., $\text{GdCl}_2(\text{H}_2\text{O})_6^+$, but these models do not account for the ARDF obtained for solution B.

Our attempts to model the stereochemistry of the solute species in solution A, e.g., $\text{Gd}(\text{H}_2\text{O})_8^{3+}$, have been unsuccessful. Of the several square antiprismatic models and the triangular dodecahedral models that we have considered, all

Table III. A Pseudocubic Model of $\text{Cl}_2\text{Gd}(\text{H}_2\text{O})_6^+$

Atom pair	Distance, Å	No.	Peak in ARDF
$\text{O}_a \cdots \text{O}_b$	2.7	2 per O	<i>a</i>
$\text{Cl}_a \cdots \text{O}_a$	3.1	3 per Cl_{is}	2
$\text{O}_a \cdots \text{O}_c$	3.9	2 per O	3
$\text{Cl}_a \cdots \text{O}_d$	4.0	3 per Cl_{is}	3
$\text{Cl}_c \cdots \text{Cl}_a$	4.1	1 per Cl_{os}	3
$\text{Cl}_c \cdots \text{O}_a$	4.1	3 per Cl_{os}	3
$\text{O}_a \cdots \text{O}_d$	4.7	1 per O	4
Gd-Cl (ion pair)	5.0	1 per Cl_{os}	4
$\text{Cl}_a \cdots \text{Cl}_b$	5.6	1 per Cl_{is}	<i>a</i>
$\text{Cl}_c \cdots \text{O}_b$	6.7	3 per Cl_{os}	6
$\text{Cl}_b \cdots \text{Cl}_c$	7.0	1 per Cl_{os}	6
$\text{Cl}_c \cdots \text{Cl}_d$	7.0	<i>b</i>	6
$\text{Cl}_c \cdots \text{Cl}_e$	10.0	<i>b</i>	<i>a</i>

^a A peak in the ARDF does not occur at this distance. ^b The number of times these interactions occur in the ARDF is dependent upon chloride simultaneously occupying these sites in the second coordination sphere.

of these models predict large peaks which do not appear in the ARDF of this solution, and none account for all of the peaks which do appear. A cubic model of $\text{Gd}(\text{H}_2\text{O})_8^{3+}$ with the chlorides located at sites adjacent to the edges of the cube also cannot account for the ARDF. The cubic model of $\text{Gd}(\text{H}_2\text{O})_8^{3+}$ with the outer-sphere chlorides located adjacent to faces of the inner polyhedron is consistent with the ARDF of solution A, except that it cannot account for the peak observed at ca. 6.0 Å. This model represents a possible description of the solute species in solution A only if it is assumed that P5 is not due to "rigid" solute structuring, and this assumption cannot be justified.

Consequently it may be concluded that the model described in Figure 5 is consistent with the ARDF of solution B but that no model has been found which accounts for the average solute species found in solution A.

Conclusions

In concentrated aqueous solutions, with and without added hydrochloric acid, Gd^{3+} is eight-coordinated. In the aqueous solution, $\text{Gd}(\text{H}_2\text{O})_8^{3+}$ is the average cationic species, and the Gd-O bond distance is ca. 2.37 Å. In the presence of a large excess of hydrogen chloride, $\text{Cl}_2\text{Gd}(\text{H}_2\text{O})_6^+$ is the average species, and the inner-sphere Gd-Cl bond distance is ca. 2.8 Å. Ion-pair Gd-Cl bond distances are ca. 4.8 Å in the aqueous solution and ca. 5.0 Å in the acidic solution. A pseudocubic model of $\text{Cl}_2\text{Gd}(\text{H}_2\text{O})_6^+$ represents a plausible description of the stereochemistry of this species, but no model of $\text{Gd}(\text{H}_2\text{O})_8^{3+}$ is consistent with all of the peaks observed in the ARDF of the aqueous solution.

In aqueous and acidic solutions of LaCl_3 and LaBr_3 , only $\text{La}(\text{H}_2\text{O})_8^{3+}$ is found, even when the solute is 10.0 N hydrochloric acid.^{16,17} That inner-sphere Gd-Cl bonding occurs in solution B indicates that chloride ion is a far better coordinating ligand toward $\text{Gd}_{\text{aq}}^{3+}$ than toward $\text{La}_{\text{aq}}^{3+}$. The different ligand affinities observed for Gd^{3+} and La^{3+} in these very concentrated solutions are consistent with the "different" Raman spectra observed for GdX_3 and LaX_3 solutions.⁵ That inner-sphere Gd-Cl bonding occurs in solution B, while no La-Cl inner-sphere bonding occurs in a similar solution, may be explained in two plausible ways: (a) Gd^{3+} , with a significantly larger ionic potential than La^{3+} , is better able to polarize and subsequently to bond to chlorides; and/or (b) the 4f electrons of Gd^{3+} are involved in and necessary for the Gd-Cl inner-sphere bonding. It is, however, beyond the scope of the x-ray diffraction experiments to validate either or both of these speculations.

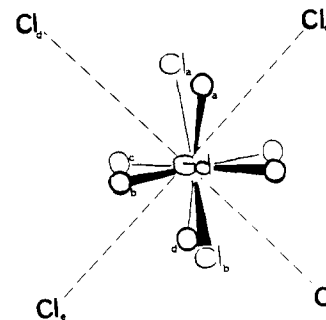


Figure 5. A pseudocubic model of $\text{Cl}_2\text{Gd}(\text{H}_2\text{O})_6^+$. The inner-sphere Gd-O distance is 2.37 Å, and the inner-sphere Gd-Cl distance has been assumed to be ca. 2.8 Å.

The extent to which structural details obtained from these very concentrated solutions may be extrapolated to dilute solutions is unknown.

Acknowledgment. Support from the Research Corporation and the National Aeronautics and Space Administration is gratefully acknowledged.

References and Notes

- (1) K. Aijisaka and M. Kainosho, *J. Am. Chem. Soc.*, **97**, 330 (1975).
- (2) R. Jones, R. A. Dwek, and S. Forsen, *Eur. J. Biochem.*, **47**, 271 (1974).
- (3) V. E. Plyushchev et al., *Zh. Neorg. Khim.*, **20**, 60 (1975).
- (4) G. Schwarzenbach and R. Gat, *Helv. Chim. Acta*, **39**, 1589 (1956).
- (5) T. Mioduski and S. Slekierski, *J. Inorg. Nucl. Chem.*, **37**, 1647 (1975).
- (6) G. W. Brady, *J. Chem. Phys.*, **33**, 1079 (1960).
- (7) E. V. Sayre, *J. Chem. Phys.*, **28**, 109 (1957).
- (8) I. I. Antipova and I. I. Kutsenko, *Zh. Neorg. Khim.*, **9**, 615 (1964).
- (9) L. O. Morgan, *J. Chem. Phys.*, **38**, 2788 (1963).
- (10) F. H. Spedding, M. J. Pikal, and B. O. Ayers, *J. Phys. Chem.*, **70**, 2440 (1966).
- (11) G. Geier and U. Karlen, *Helv. Chim. Acta*, **54**, 135 (1971).
- (12) A. Fratiello, V. Kubo, S. Peak, B. Sanchez, and R. E. Schuster, *Inorg. Chem.*, **10**, 2552 (1971).
- (13) F. H. Spedding and W. C. Mundy, *J. Chem. Phys.*, **59**, 2183 (1973).
- (14) V. V. Bakakin, R. F. Klevstova, and L. P. Solov'eva, *Zh. Strukt. Khim.*, **15**, 820 (1974).
- (15) W. H. Zachariasen, M. Marezio, and H. A. Plettinger, *Acta Crystallogr.*, **14**, 234 (1961).
- (16) L. S. Smith and D. L. Wertz, *J. Am. Chem. Soc.*, **97**, 2365 (1975).
- (17) L. S. Smith and D. L. Wertz, submitted for publication.
- (18) J. L. Hoard, B. Lee, and M. D. Lind, *J. Am. Chem. Soc.*, **87**, 1612 (1965).
- (19) T. Moeller and R. Ferrus, *J. Inorg. Nucl. Chem.*, **20**, 261 (1961).
- (20) G. R. Choppin and S. L. Bertha, *Inorg. Chem.*, **8**, 613 (1969).
- (21) L. A. K. Staveley, D. R. Markham, and M. R. Jones, *J. Inorg. Nucl. Chem.*, **30**, 231 (1968).
- (22) F. H. Spedding, P. F. Cullen, and A. Haben Schuss, *J. Phys. Chem.*, **78**, 1106 (1974).
- (23) R. C. Agarwal, *J. Indian Chem. Soc.*, **51**, 772 (1974).
- (24) F. H. Spedding et al., *J. Chem. Phys.*, **60**, 1578 (1974).
- (25) I. M. Batyayev and R. S. Fogileva, *Zh. Neorg. Khim.*, **19**, 670 (1974).
- (26) L. J. Nugent et al., *J. Phys. Chem.*, **77**, 1528 (1973); *J. Inorg. Nucl. Chem.*, **37**, 1767 (1975).
- (27) F. H. Spedding, J. A. Rard, and V. W. Saeger, *J. Chem. Eng. Data*, **19**, 373 (1974).
- (28) T. Goto and M. Smutz, *J. Inorg. Nucl. Chem.*, **27**, 663 (1965).
- (29) D. F. Peppard, G. W. Mason, and I. Hucker, *J. Inorg. Nucl. Chem.*, **24**, 881 (1961).
- (30) G. R. Chopin, D. E. Henrie, and K. Bajis, *Inorg. Chem.*, **5**, 1743 (1966).
- (31) B. G. Wybourne, "Spectroscopic Properties of the Rare Earths", Wiley, New York, N.Y., 1965.
- (32) J. Foos, A. S. Kertes, and M. E. Peleg, *J. Inorg. Nucl. Chem.*, **36**, 837 (1974).
- (33) D. L. Nelson and D. E. Irish, *J. Chem. Phys.*, **54**, 4479 (1971); *J. Chem. Soc., Faraday Trans. 1*, **69**, 156 (1973).
- (34) D. G. Karraker, *Inorg. Chem.*, **7**, 473 (1968).
- (35) I. M. Batyayev et al., *Zh. Neorg. Khim.*, **16**, 66 (1971); **18**, 1451 (1973).
- (36) E. I. Chubakova and N. A. Skorik, *Zh. Neorg. Khim.*, **18**, 1446 (1973).
- (37) R. J. Hinchey and J. W. Cobble, *Inorg. Chem.*, **9**, 917 (1970).
- (38) G. R. Choppin and P. J. Unrein, *J. Inorg. Nucl. Chem.*, **25**, 387 (1965).
- (39) N. N. Kozachenko and I. M. Batyayev, *Zh. Neorg. Khim.*, **15**, 888 (1970); **16**, 66, 125, 1841 (1971); **18**, 938 (1973).
- (40) N. K. Davidenko, L. N. Lugina, and K. P. Yatsimirskii, *Zh. Neorg. Khim.*, **17**, 104 (1972); **18**, 1453 (1973).
- (41) R. F. Kruh, *Chem. Rev.*, **62**, 319 (1962).
- (42) $\sigma = (\text{total counts})^{-1/2} \times 100$ at each of the 219 data points.
- (43) B. D. Cullity, "Elements of X-ray Diffraction", Addison-Wesley, Reading, Mass., 1956, p 172.
- (44) H. A. Levy, M. D. Danford, and A. H. Narten, Report No. 3960, Oak Ridge National Laboratories, Oak Ridge, Tenn., 1966.
- (45) B. E. Warren, "X-ray Diffraction", Addison-Wesley, Reading, Mass., 1969.

- p 145.
 (46) F. Hajdu, *Acta Crystallogr., Sect. A*, **27**, 73 (1971); G. Palinkas, *ibid.*, **29**, 10 (1973).
 (47) F. Hajdu, *Acta Crystallogr., Sect. A*, **28**, 250 (1972), and private communications.
 (48) R. M. Lawrence and R. F. Kruh, *J. Chem. Phys.*, **41**, 4758 (1967).
 (49) J. H. Konnert and J. Karle, *Acta Crystallogr., Sect. A*, **29**, 702 (1973).
 (50) J. Waser and V. Schomaker, *Rev. Mod. Phys.*, **25**, 671 (1953).
 (51) D. L. Wertz and J. R. Bell, *J. Inorg. Nucl. Chem.*, **35**, 137, 861 (1973).
 (52) D. H. Templeton and C. H. Dauben, *J. Am. Chem. Soc.*, **75**, 6069 (1953).
 (53) P. Polx, *C. R. Acad. Sci., Ser. C*, **270**, 1852 (1970).
 (54) $n_1 = 7.6 \times 10^3 e^2 / 9.5 \times 10^2 e^2 = 8.0$.
 (55) Assuming $n_1 + n_2 = 8$, then $n_1 \approx 6.0$ and $n_2 \approx 2.0$ to satisfy the relationship $1.05 \times 10^4 e^2 = n_1 \times 9.5 \times 10^2 e^2 + n_2 \times 2.4 \times 10^3 e^2$.
 (56) S. C. Lee and R. Kaplow, *Science*, **169**, 477 (1970).
 (57) D. L. Wertz, *J. Solution Chem.*, **1**, 489 (1972).
 (58) R. M. Lawrence and R. F. Kruh, *J. Chem. Phys.*, **47**, 4758 (1967).
 (59) D. L. Wertz and R. F. Kruh, *J. Chem. Phys.*, **50**, 4313 (1969).
 (60) J. N. Albright, *J. Chem. Phys.*, **56**, 3783 (1972).
 (61) J. R. Bell and D. L. Wertz, *J. Am. Chem. Soc.*, **95**, 1456 (1973).
 (62) J. L. Tyvoll and D. L. Wertz, *J. Inorg. Nucl. Chem.*, **36**, 3713 (1974).

Quadrupole Coupling Constants of Square-Planar Copper(II)-Sulfur Complexes from Single-Crystal Electron Paramagnetic Resonance Spectroscopy

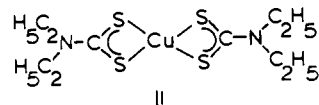
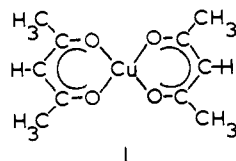
Lawrence K. White and R. Linn Belford*

Contribution from the Department of Chemistry, University of Illinois, Urbana, Illinois 61801. Received September 2, 1975

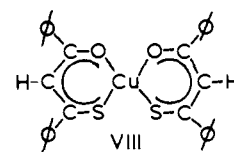
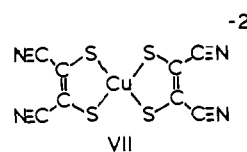
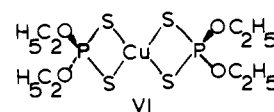
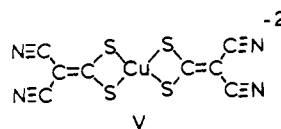
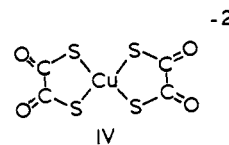
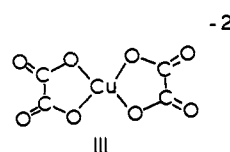
Abstract: The nuclear quadrupole coupling parameters are measured for copper in six square-planar complexes, five having sulfur donor atoms and one having both sulfur and oxygen donors. Computer simulations of the EPR spectra of the Cu-doped powders are employed to refine the principal g and A values. The secondary ($\Delta m_I = 1$) transitions of the EPR spectra of Cu-doped single crystals are analyzed for the quadrupole coupling parameters. The small quadrupole coupling constant for the Cu-S₄ complexes ($QD \approx 0.7 \times 10^{-4} \text{ cm}^{-1}$) implies an effectively spherical symmetry which is attributed chiefly to the large covalent character of the Cu-S σ bond. A few anomalies are observed in the quadrupole data. A larger quadrupole coupling constant is observed for diethyl dithiophosphate, Cu(S₂P(OC₂H₅)₂)₂, than for other Cu-S₄ complexes studied, i.e., $1.8 \times 10^{-4} \text{ cm}^{-1}$ compared to $0.7 \times 10^{-4} \text{ cm}^{-1}$. Also, a large asymmetry parameter (QE) is observed for the bis(maleonitriledithiolate) cuprate(II), Cu(mnt)₂²⁻, dianion and the mixed S-O square-planar complex copper(II) bis(*cis*-monothiodibenzoylmethanate), Cu(SdbmO)₂. The quadrupole coupling parameters may be sensitive to Cu-P transannular interaction in Cu-(S₂P(OC₂H₅)₂) and to the strong complex π bonding present in Cu(mnt)₂²⁻.

I. Introduction

In the early 1950's Bleaney¹⁻³ suggested that quadrupole coupling data could be obtained from single-crystal EPR studies. So and Belford^{4,5} examined the secondary (or forbidden $\Delta m_I = \pm 1$) transitions in the single-crystal EPR spectra of several Cu-O complexes, including four square-planar β -ketoenolates (typified by Cu(acac)₂, bis(2,4-pentanedionato)copper(II), I) and one square-planar copper(II)-sulfur complex (Cu(dtc)₂, bis(diethyl dithiocarbamate)copper(II), II). Recently we reported⁶ the quadrupole coupling



constant of another square-planar Cu-O complex (Cu-(C₂O₄)₂²⁻, bis(oxalato)cuprate(II) dianion, III). These studies have been continued. Here we study several copper(II)-sulfur complexes of square-planar geometry to determine the sensitivity of the quadrupole coupling parameter to more subtle aspects of the electronic structures of the molecules. The quadrupole coupling parameters are obtained from the single-crystal EPR spectra for five square-planar Cu-S complexes: Cu(dto)₂²⁻, bis(dithiooxalate) cuprate(II), IV; Cu(i-mnt)₂²⁻, bis(1,1-dicyano-2,2-dithioethylene)cuprate(II), V; Cu(dtc)₂²⁻, II, EPR data repeated; Cu(S₂P(OC₂H₅)₂)₂, bis(diethyl dithiophosphate)copper(II) (in Ni host), VI; and Cu(mnt)₂²⁻, bis(1,2-dicyano-1,2-dithioethylene)cuprate(II), VII. We also report data for one mixed sulfur-oxygen donor



complex Cu(SdbmO)₂, copper(II) bis(*cis*-monothiodibenzoylmethanate) (VIII).

We have employed EPR data obtained from computer simulation of powdered samples to help analyze the single-crystal EPR spectra for these nearly axial systems. The features of the EPR spectrum of a powder are extremely sensitive to the magnitude of the principal g and A values; easily obtainable precisions are ± 0.0003 for g and $\pm 0.3 \times 10^{-4} \text{ cm}^{-1}$ for A . Since the hyperfine interaction in these compounds is much larger than either the nuclear Zeeman or nuclear quadrupole interaction, neither the line positions nor intensities of the primary ("allowed" $\Delta m_I = 0$) transitions are affected substantially by these interactions. Only the electronic Zeeman